Original Paper

Cellular Physiology and Biochemistry

Cell Physiol Biochem 2004;14:23-30

Accepted: September 02, 2003

A Novel Non-Neuronal *h*SK3 Isoform with a Dominant-Negative Effect on *h*SK3 Currents

Oliver H. Wittekindt[1,2], Tobias Dreker[1], Deborah J. Morris-Rosendahl[2], Frank Lehmann-Horn[1] and Stephan Grissmer[1]

[1]Department for Applied Physiology, University-Ulm, [2]Institute for Human Genetics and Anthropology, Albert-Ludwigs-University Freiburg

Key Words

Potassium channel • Alternative splicing • SK3 • KCNN3

Abstract

We have identified a *h*SK3-transcript, *h*SK3_ex1c, which is generated by alternative splicing. Isoform *h*SK3_ex1c lacks the cytosolic N-terminus and the first transmembrane helix and is exclusively expressed in non-neuronal tissues. *h*SK3 transfected tsA cells showed a Ca^{2+}-activated K^+ current in patch-clamp experiments, whereas *h*SK3_ex1c transfected cells and cells co-transfected with both isoforms did not. We fused both isoforms to fluorescence proteins and observed *h*SK3 localization predominantly in the plasma membrane. The co-expression of *h*SK3 + *h*SK3_ex1c resulted in their cytoplasmic co-localization. Thus, *h*SK3_ex1c has a dominant-negative effect on *h*SK3 by preventing its transport into the plasma membrane.

Introduction

Small conductance calcium-activated potassium channels (SK channels) form a distinct subfamily of potassium channels, which comprises three members, SK1 to SK3 [1]. Their subunits have six transmembrane helices, a P-loop region between the fifth and sixth transmembrane helix and cytosolic N- and C-terminal regions. All members are voltage-independent and their activation by elevated cytosolic Ca^{2+} concentrations is mediated via calmodulin [2-5]. They are involved in modulating neuronal firing [6, 7].

Alternative splicing is assumed to increase the functional diversity of potassium channels and might also be involved in the regulation of whole-cell current amplitude [8]. Alternative splicing within the SK channel subfamily has been shown only for SK1 [9, 10] and SK3 channels [11, 12]. In the case of SK3 channels two isoforms have been described. One isoform shows an altered outer pore region which changes its pharmaco-kinetic properties [12]. The other one lacks a cytosolic N-terminal region and the first transmembrane helix. This isoform is shown to have a dominant-negative regulatory effect on SK channels [11] and is shown to be expressed in neuronal tissues.

Here we describe an additional non-functional *h*SK3-isoform, *h*SK3_ex1c, which is generated by alternative splicing and is co-expressed with *h*SK3 in lymphocytes, lung and skeletal muscle but contrary to the isoform previously reported by Tomita et al. [11], *h*SK3_ex1c is absent in neuronal tissues. Since this isoform is shown to have a dominant-negative effect on

KARGER

Fax +41 61 306 12 34
E-Mail karger@karger.ch
www.karger.com

1015-8987/04/0142-0023$17.50/0

Accessible online at:
www.karger.com/journals/net

Prof. Dr. Stephan Grissmer
Department of Applied Physiology, University Ulm
Albert-Einstein-Allee 11, 89081 Ulm (Germany)
Tel. +49 (0)731 5023253, Fax +49 (0)731 5023260
E Mail stephan.grissmer@medizin.uni-ulm.de

*h*SK3, it possibly regulates SK3-channel activity in non-neuronal tissues.

Materials and Methods

If not assigned otherwise, all standard chemicals were obtained from Sigma (Germany). Scyllatoxin was obtained from Latoxan (France).

RT-PCR

Reverse transcription (RT) was carried out on 2 µg of total RNA from adult and fetal whole brain, lung, heart, skeletal muscle (Research Genetics) and a B-lymphocyte cell line (extracted using the RNeasy extraction kit, Qiagen) using superscript II (Invitrogen) according to manufacturer's protocol. Furthermore, as an additional template, a cDNA library from six to eight week old whole human embryos (gift from Dr. Francis Poulat, CNRS France) was used. *h*SK3_ex1c transcripts were amplified using the primers II1-F1 (cctgccacgcgacatctg) and R10 (gacacctttcccacagtatg) and *h*SK3 transcripts with the primers *h*SK3-F (gctctcttggggtttgt) and R10. Primers GAPDH-F (gggcgcctggtcaccacgg) and GAPDH-R (ctgatgatcttgacgctgttg) were used as controls for the RT reaction and to test for any contaminating genomic DNA. PCR was carried out in a RT reaction mix without RNA, water and genomic DNA as a negative control.

cDNA construction

IMAGE clone 686525 was obtained from a cDNA library from human tonsillar cells, which were enriched for B cells and was distributed by the RZPD (AA255937, resource centre of the German human genomic project, RZPD: IMAGp998C061678). The entire coding region of isoform *h*SK3_ex1c was amplified from the IMAGE clone 686525 using the primers *h*SK3_1c-F1 (aaaaactcgagccaccatggagagacctataaaggac) and *h*SK3-R1 (aaaatggatccccgcaactgcttgaacttgtgta) and cloned into pDsRED2-N1 (Clontech) via XhoI/BamHI sites. It encodes the fusion protein *h*SK3_ex1c-DsRED. The entire coding region of *h*SK3 was amplified with the primers *h*SK3-F1 (aaaatggatccccgcaactgcttgaacttgtgta) and *h*SK3-R1 and cloned via BamHI/XhoI into pEGFP-N1 (Clontech). It encodes the fusion protein *h*SK3-eGFP. In *h*SK3_ex1c-DsRED and *h*SK3-eGFP the fluorescent protein is fused to the C-terminal region of *h*SK3 and *h*SK3_ex1c. The N-terminal coding part of *h*SK3_ex1c was isolated by HindIII/SfiI digestion from clone *h*SK3_ex1c-DsRED and was used to replace the HindIII/SfiI fragment in the clone pHygro-*h*SK3Q19 (a gift from Dr. Heike Jäger, University of Ulm) in order to generate an untagged *h*SK3_ex1c construct.

Cell culture

tsA201 cells (tsA cells), a HEK cell line stably transfected with the SV40 T-antigen (formerly called s93/tsA1609neo) were used for all experiments [13, 14]. tsA cells were cultured in MEM medium containing glutamax-I and Earle's salts (GIBCO, Germany) and 10 % fetal bovine serum. A mixture of 0.5 µg plasmid DNA encoding pEGFP-N1 (Clontech) and 2 µg of plasmid DNA (pHygro-*h*SK3_ex1c and pHygro-*h*SK3Q19) were transfected into tsA cells using FUGENE 6 (Roche) according to the manufacturer's protocol. Plasmids *h*SK3_ex1c-DsRED and *h*SK3-eGFP were transfected without any transfection marker. Three to four days after transfection, cells were suspended and transferred to poly-lysine coated glass slides prior to further usage.

Patch-clamp experiments

Experiments were carried out using the whole-cell recording mode of the patch-clamp technique [15]. Electrodes were pulled from glass capillaries in two stages and fire-polished to resistances of 3.5 to 4 MΩ when filled with internal solution (in mM: 135 potassium aspartate, 2 $MgCl_2$, 10 HEPES, 10 EGTA and 8.7 $CaCl_2$ corresponding to $[Ca^{2+}]_{free}$ of 1 µM, pH 7.2). Membrane currents were measured with an EPC-9 amplifier (HEKA elektronik, Germany) using Pulse and Pulsefit (HEKA elektronik, Germany) as acquisition and analysis software. The cytosolic Ca^{2+}-concentration was adjusted to $[Ca^{2+}]_{free}$ = 1 µM by whole-cell dialysis with internal solution. Na^+-solution (in mM: 160 NaCl, 4.5 KCl, 2 $CaCl_2$, 1 $MgCl_2$, 5 HEPES, pH 7.4) and K^+-solution (in mM: 164.5 KCl, 2 $CaCl_2$, 1 $MgCl_2$, 5 HEPES, pH 7.4) were used as external solutions. The membrane potential was held at -80 mV (in Na^+-solution) or 0 mV (in K^+-solution), clamped to -120 mV for 50 ms followed by 400 ms ramps from -120 to +60 mV. In between ramps the potential was clamped again to -80 mV (in Na^+-solution) or 0 mV (in K^+-solution). Whole-cell conductance was calculated from the slope of the ramp current measured between -90 mV to -70 mV. The whole-cell conductance observed in the presence of Na^+-solution was presumed as background conductance and therefore subtracted from those conductances, found in the presence of K^+-solution with and without scyllatoxin (ScTX). The fractional conductance was defined as the ratio between the conductance found in K^+-solution and the conductance observed in K^+-solution with and without ScTX. Data are given as mean ± SEM.

Intracellular localization of hSK3-isoforms

Cells were washed with PBS buffer and were observed in PBS buffer without any fixation. For selecting cells, fluorescence was excited using a 100 W mercury lamp. GFP and DsRED fluorescence were assessed independently (GFP: Excitation 465 nm, band width 15 nm ; emission 520 nm, long pass filtered; DsRED: Excitation 520 nm, band width 20 nm; emission 630 nm, band width 30 nm). Confocal assessment was carried out using the Laser Scanning System Radiance 2000 (Biorad) attached to an inverted Microscope (Nikon Eclipse TE300, Nikon). A PlanApo 60X oil objective (Nikon) was used for all confocal measurements. Data recording and analyses were carried out using the Lasersharp 2000 software package (Biorad). GFP fluorescence was excited with the 488 nm line of an argon laser and emission was measured using an HQ510/30 filter (Nikon). DsRED fluorescence was excited with the 543 nm line of a green HeNe-laser and emitted light was long pass filtered using a E600/LP filter (Nikon).

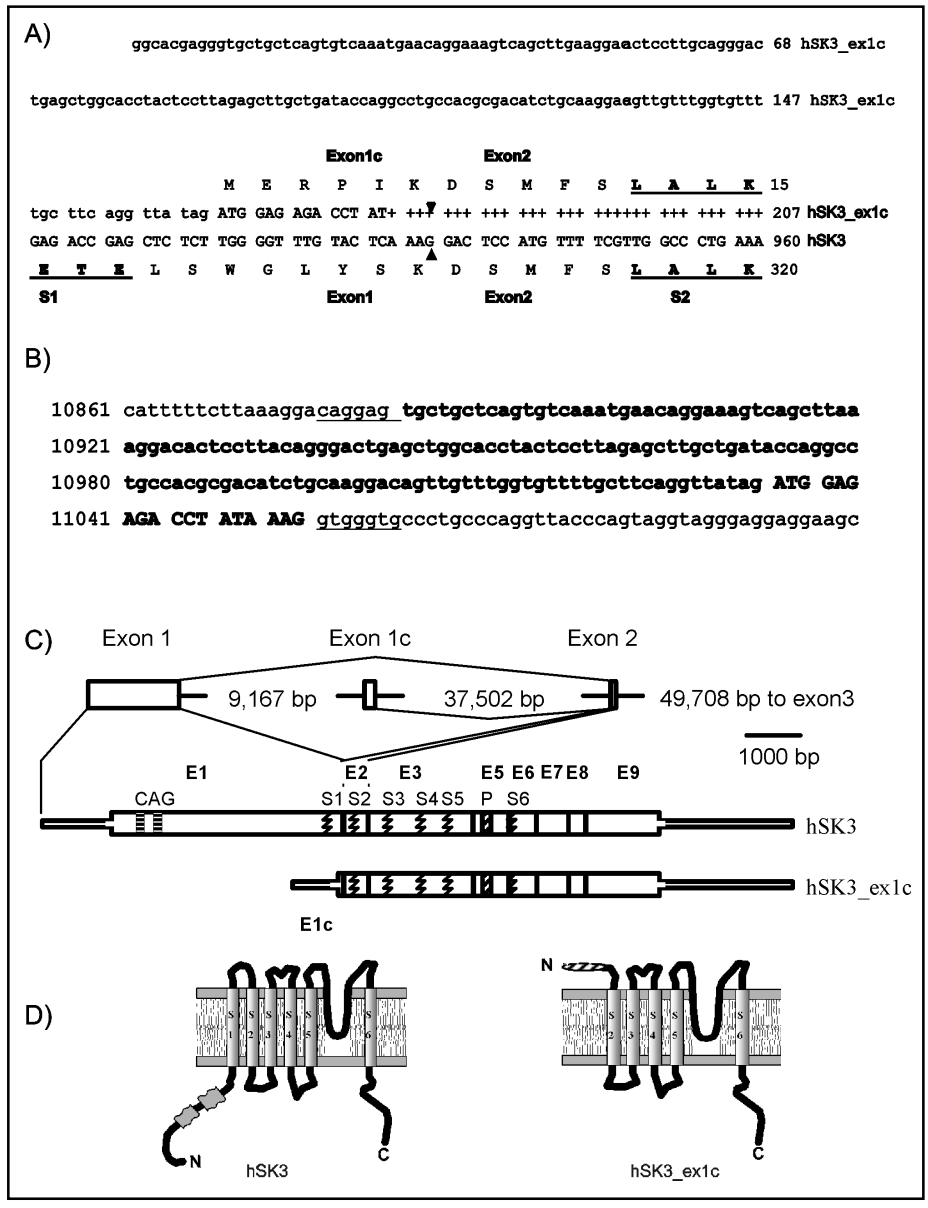

Fig. 1. Isoform *h*SK3_ex1c is generated by alternative splicing. A) cDNA and protein sequence comparison of *h*SK3 and *h*SK3_ex1c. Small letters represent untranslated and capital letters translated regions. Identical nucleotides are shown as + and exon boundaries with arrowheads. Exons 1, 2, and 1c are assigned. Protein sequences according to the shown cDNA regions are given. Amino acids within the transmembrane helices S1 and S2 are shown in bold letters and are underlined. B) Genomic sequence spanning exon 1c. The cDNA region from positions 10 to 180 (shown as bold letters) is flanked by typical splice acceptor and donor sites (underlined). C) Organization of the genomic region spanning exons 1, 1c, and 2 and a scheme for alternative splicing. Distances between the exons are given. Schemes for both cDNAs are shown below. Broad boxes represent the ORF and narrow boxes the UTRs. The Exons (E1, E1c, to E9), both CAG repeats and transmembrane helices S1 to S6 and the P-loop are shown. D) Presumed topology of *h*SK3 and *h*SK3_ex1c subunits.

Results

The insert of IMAGE clone 686525 spanned 1984 bp. Its sequence is identical to the original known *h*SK3 sequence (Accession no.: AJ251016) 3' from position 928 of the *h*SK3 ORF but it differs 5' from this position (Figure 1A). Except for a 10 bp region from the 5' end of the IMAGE clone, the differing cDNA sequence overlaps with the genomic sequence (Accession No.: AF336797) from positions 10882 to 11052 and is flanked by typical splice acceptor and donor sites (Figure 1B). The remaining 10 bp 5' region of the cDNA could not be detected in the genomic sequence, neither by blast search, nor by sequence comparison with the sequence of the *h*SK3/*KCNN3* gene (AF336797). This might indicate that there may be an additional, still unknown exon within the *h*SK3/*KCNN3* gene. The detected transcript represented by IMAGE clone 686525 was generated by alternative splicing and we have named it *h*SK3_ex1c (Figure 1C). The longest ORF in the newly identified cDNA starts at position 163 (Figure 1A) and encodes an *h*SK3 isoform that lacks the first transmembrane helix and the cytosolic N-terminal region of *h*SK3 (Figure 1D). Its extracytosolic region is 7 amino acids longer than that of *h*SK3-1B [11].

The expression of *h*SK3 and *h*SK3_ex1c was investigated by RT-PCR (Figure 2). Transcripts encoding *h*SK3 were observed in all tissues tested as well as in the human embryonic cDNA library. Contrary to this, *h*SK3_ex1c transcripts were only observed in lung, skeletal muscle and the B-lymphocyte cell line, but were

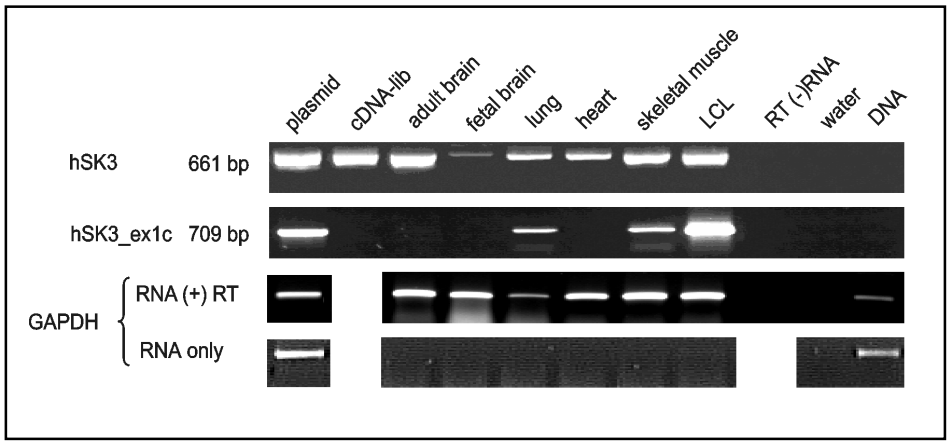

Fig. 2. Expression of *h*SK3 and *h*SK3_ex1c isoforms using RT-PCR. The expected fragment length of the PCR products and the transcripts' names are given on the left hand side. RNA sources are given above each lane (cDNA: cDNA library form six- to eight-week old human embryos, LCL: lymphocyte cell line). Plasmid DNA (plasmid) was used as positive control. PCR was carried out on the reverse transcriptase reaction mix without RNA (RT(-)RNA), water, and genomic DNA (DNA) were negative controls. In order to confirm the reverse transcriptase reaction, PCRs were carried out using glycerin-aldehyde-dehydrogenase specific primers (GAPDH; RNA(+)RT). Since these primers also amplify genomic DNA, they were used to test for contaminating genomic DNA (GAPDH; RNA only) using the tested RNAs without prior reverse transcriptase reaction as a template.

absent in the cDNA library derived from 6 to 8-week old human embryos, heart, fetal and adult brain. Therefore we were interested in the functional properties of the newly identified isoform.

Since both isoforms were shown to be co-expressed in several tissues we also investigated the effect of *h*SK3_ex1c expression on *h*SK3, by co-expressing them in tsA cells (Figure 3). The data represent results from three independent transfection experiments. tsA cells expressing isoform *h*SK3 alone showed a whole-cell conductance of 1.6 ± 0.3 nS (n=7) with Na^+-solution as bath solution, which was increased to 5.4 ± 1.2 nS (n=7) when the external solution was exchanged to K^+-solution. Current amplitudes corresponding to much higher whole-cell conductances were described in a previous report for rSK3 expressing HEK293 cells [16]. Even in this study the published current amplitudes varied between different experiments. Therefore, the comparable low current amplitudes observed here are most likely due to the applied expression system. In the presence of 10 nM ScTX in K^+-solution, a mean whole-cell conductance of 1.9 ± 0.4 nS (n=7) was observed.

Whole-cell conductances found with Na^+-solution as external solution were assumed to be background conductances and were therefore subtracted from those observed in K^+-solution with and without ScTX. After subtracting the background conductance, the fraction of remaining conductance in the presence of 10 nM ScTX in K^+-solution was calculated as the fraction of whole-cell conductance with K^+-solution as bath solution to be 0.22 ± 0.04 nS (n=7). *h*SK3_ex1c expressing cells showed a whole-cell conductance of 0.6 ± 0.1 nS (n=12) in Na^+-solution which did not significantly increase in K^+-solution (0.8 ± 0.1 nS; n=12). A similar situation was observed, when tsA cells co-expressed both isoforms (whole-cell conductance of 0.4 ± 0.1 nS; n=12 for Na^+-solution and 0.6 ± 0.1 nS; n=12 for K^+-solution). This indicates, that the isoform *h*SK3_ex1c is able to reduce SK3 currents, if it is co-expressed with the functional *h*SK3 isoform. A similar effect was described for the *h*SK3-1B isoform [11]. In that case it was shown that *h*SK3-1B was able to trap *h*SK3 subunits in the cytoplasm, which could explain the reduction of SK3 whole-cell currents. We assumed a similar mechanism for the isoform *h*SK3_ex1c described here. Therefore we investigated the intracellular localization of *h*SK3 and *h*SK3_ex1c. We fused both isoforms at their C-termini to different fluorescent proteins and expressed them in tsA cells (Figure 4). The data represent the results from two independent transfection experiments. Cells expressing isoform *h*SK3 fused to eGFP (*h*SK3-eGFP) showed a whole-cell conductance of 21.2 ± 8.2 nS (n=13) with Na^+-solution and 63.0 ± 16.4 nS (n=13) with K^+-solution as external solutions. This conductance in K^+-solution was reduced by 10 nM ScTX (27.1 ± 8.8 nS; n=13), that corresponds to a fractional conductance of 0.16 ± 0.04 (n=13) of the remaining current, when the background conductance is subtracted. Interestingly, the whole-cell conductance of cells expressing *h*SK3-eGFP was strongly increased compared to those cells expressing the wild type *h*SK3 without the fused GFP. Cells expressing isoform *h*SK3_ex1c-DsRED (*h*SK3_ex1c fused with its C-term to DsRED) did not show any increased whole-cell conductance after changing the bath solution from Na^+-solution (0.3 ± 0.1 nS; n=9) to K^+-solution (0.7 ± 0.1 nS, n=9). This, however, was the case

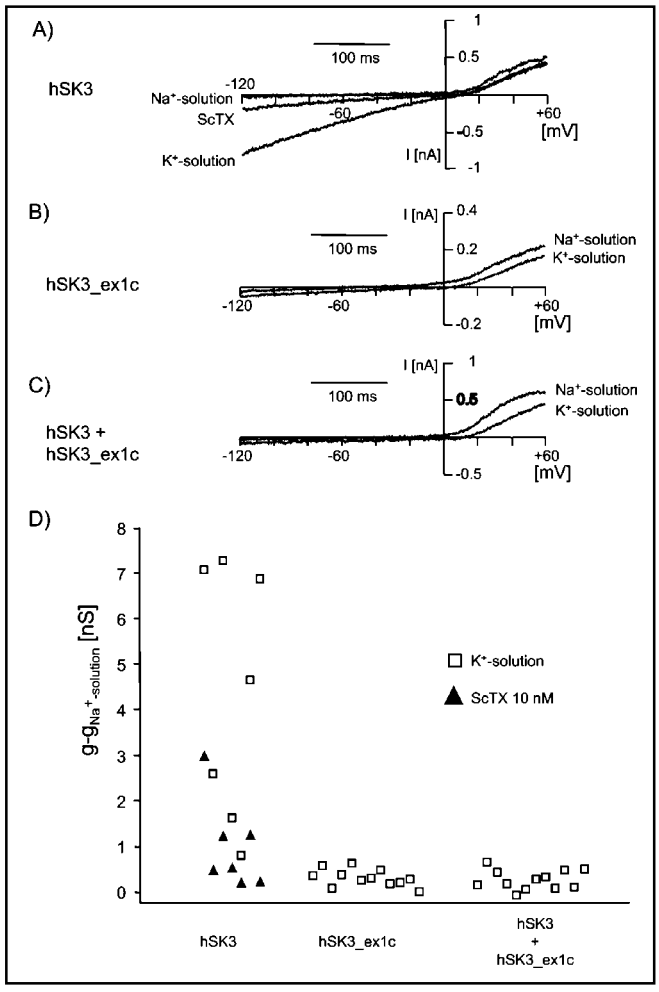

Fig 3. Expression of isoforms *h*SK3 and *h*SK3_ex1c in tsA cells. Isoforms *h*SK3 and *h*SK3_ex1c were transiently expressed in tsA cells and currents were measured in the whole-cell mode of the patch-clamp technique with 1 µM free internal Ca^{2+} and Na^+-solution and K^+-solution as external solutions. SK3 currents were blocked by adding 10 nM ScTX to K^+-solution. Representative current traces for cells expressing *h*SK3 (A), *h*SK3_ex1c (B) and for cells co-expressing both isoforms (*h*SK3 + *h*SK3_ex1c; C) are shown above. Whole-cell conductances found for each experiment are shown in diagram D. Whole-cell conductance found in Na^+-solution was assumed as background conductance and was therefore subtracted from currents measured in K^+-solution with and without 10 nM ScTX. 10 nM ScTX blocks SK3 currents. Cells expressing *h*SK3_ex1c and those co-expressing both isoforms did not show conductance above 1 nS and therefore ScTX was not tested on these cells.

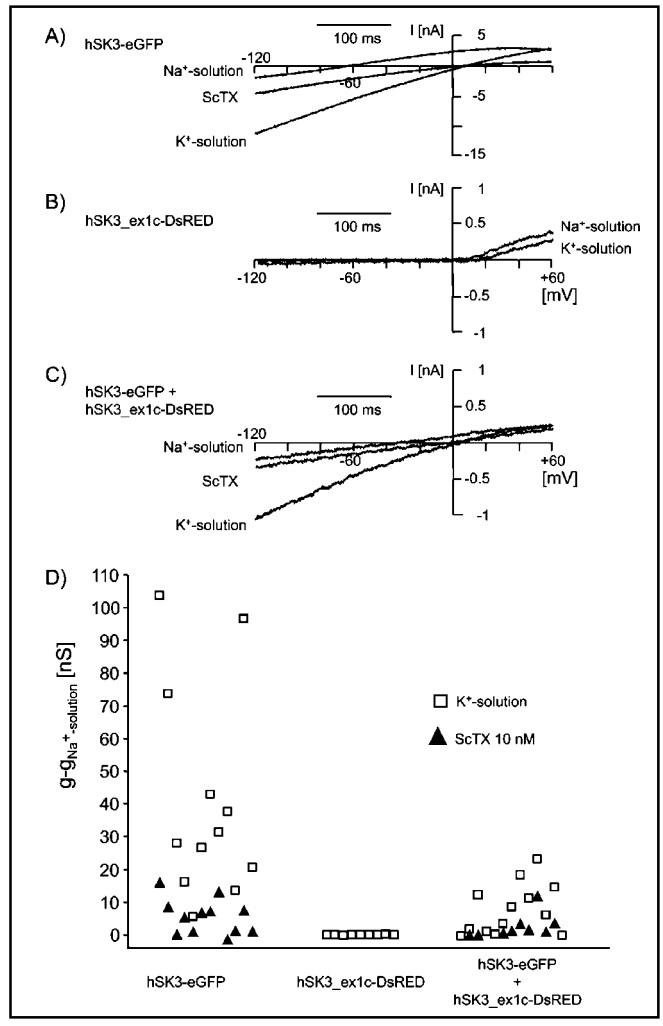

Fig 4. Expression of isoforms tagged with fluorescence proteins. Isoforms fused with their C-terms to fluorescence proteins behave the same as the wild type isoforms, when expressed in tsA cells. Currents were measured as described. Na^+- and K^+-solution with and without 10 nM ScTX were used as external solutions. Representative current traces for cells expressing *h*SK3-eGFP (A), *h*SK3_ex1c-DsRED (B) and for cells co-expressing both isoforms (*h*SK3-eGFP + *h*SK3_ex1c-DsRED; C) are shown. Whole-cell conductances for each experiment are shown in the diagram below (D). Whole-cell conductance found in Na^+-solution was subtracted from the one in K^+-solution with and without 10 nM ScTX. Cells expressing the GFP tagged isoform *h*SK3-eGFP showed conductances up to 110 nS. These currents were blocked by 10 nM ScTX. Contrary to that, cells expressing *h*SK3_ex1c-DsRED did not show any significantly increased whole-cell conductance. Cells co-expressing *h*SK3-eGFP + *h*SK3_ex1c-DsRED showed a significant whole-cell conductance in K^+-solution. These currents were blocked by 10 nM ScTX

when *h*SK3-eGFP and *h*SK3_ex1c-DsRED were co-expressed (1.9 ± 0.4 nS in Na^+-solution and 10 ± 2.7 nS in K^+-solution; n=12). The remaining whole-cell conductance in K^+-solution in the presence of 10 nM ScTX was found to be 5.5 ± 1.7 nS (n=8), which corresponds to a remaining fractional conductance of 0.14 ± 0.05 (n=8) (after subtraction of background conductance).

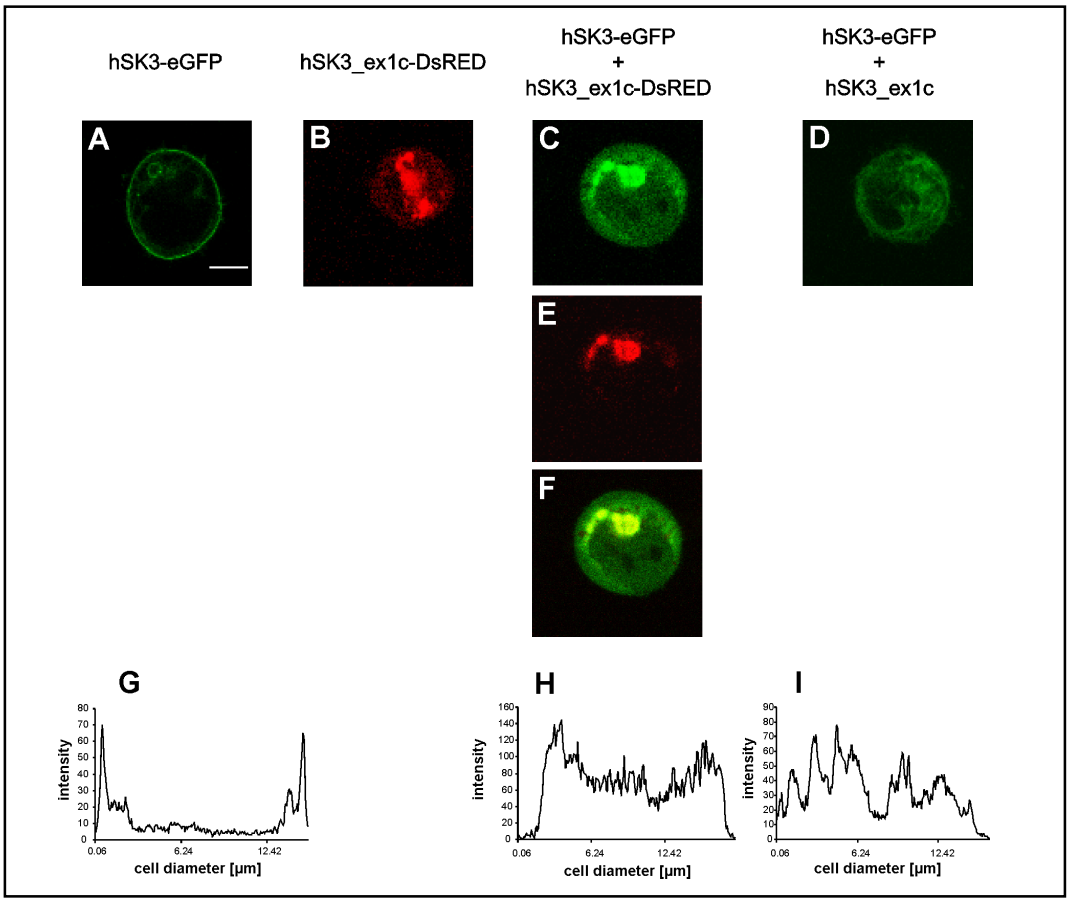

Fig 5. Intracellular localization of *h*SK3 isoforms. *h*SK3-eGFP is shown as green fluorescence in A,C and D. *h*SK3_ex1c-DsRED is shown as red fluorescence in B and E. Merged images for GFP and DsRED fluorescence of co-expressed *h*SK3-eGFP and *h*SK3_ex1c-DsRED are shown in F. The averaged intensity histograms for GFP fluorescence are shown in G-I. Thus the isoform *h*SK3_ex1c prevents *h*SK3 translocation to the plasma membrane. Scale bar 5 µm.

The mean whole-cell conductance observed for cells expressing the GFP-tagged *h*SK3 isoform, *h*SK3-eGFP, is approximately 12 fold higher compared to cells expressing wild type *h*SK3 channels. Even when *h*SK3-eGFP is co-expressed with *h*SK3_ex1c-DsRED, significant whole-cell currents were observed, which were carried by SK3 channels. This may indicate an incomplete inhibition of *h*SK3 channels by the *h*SK3_ex1c-DsRED construct. However, since the SK3 current varies strongly between different cells co-expressing the tagged isoforms, it is much more likely, that the incomplete inhibition is due to the higher expression level of functional *h*SK3-eGFP rather than to the fact that the fused fluorescence proteins interfere with subunit assembly.

The intracellular localization of *h*SK3-eGFP and *h*SK3_ex1c-DsRED were studied using confocal laser scanning microscopy (Figure 5). The fluorescent pattern of cells expressing *h*SK3-eGFP alone (Figure 5A) was strikingly different from those co-expressing *h*SK3-eGFP and *h*SK3_ex1c-DsRED (Figure 5C), or with the untagged isoform *h*SK3_ex1c (Figure 5D). Whereas *h*SK3-eGFP-expressing cells showed a sharp annular distribution of fluorescence, the co-expressing cells show a more uniform distribution. This observation is confirmed by the average intensity histograms (Figure 5G-I), which represent the average intensity along five axes drawn through the cell. The yellow colored regions in the merged images of cells co-expressing both fluorescence labeled isoforms indicated their co-localization (Figure 5F). Cells expressing the *h*SK3_ex1c-DsRED construct alone, showed an intracellular speckling fluorescence pattern that aggregates in some regions (Figure 5B). This indicates that isoform *h*SK3_ex1c is not incorporated into the plasma membrane. In contrast, such an incorporation has been shown for the functional isoform *h*SK3 (Figure 5A). In addition, *h*SK3_ex1c seems to be able to prevent the incorporation of *h*SK3 subunits into the plasma membrane, which could explain the reduction of Ca^{2+}-activated K^+ current, as has been shown for *h*SK3-1B [11].

Discussion

The recently reported isoform *h*SK3-1B was described as an isoform having a dominant-negative regulatory effect on SK currents [11]. This isoform was shown to be generated by alternative splicing and was

presumed to encode a shortened SK3 subunit, which is lacking the first transmembrane-spanning S1 helix and the cytosolic N-terminal region [11]. Here we describe a similar *h*SK3 isoform, *h*SK3_ex1c, which is also generated by alternative splicing. As in the case of *h*SK3-1B, *h*SK3_ex1c lacks a cytosolic N-terminus and the S1 helix, but contrary to *h*SK3-1B, the longest predicted ORF of *h*SK3_ex1c transcripts encodes a protein, which is extended towards its extracytosolic N-terminus by seven amino acids. Like *h*SK3-1B, *h*SK3_ex1c is able to suppress SK3 currents by trapping functional isoforms in the cytoplasm.

The physiological role of these isoforms is not yet known. An inactive isoform of a cardiac potassium channel K_vLQT_1 has been described [17]. It is assumed that this isoform could play a role as a regulator for whole-cell K_vLQT_1-current amplitude. This assumption was confirmed, since mutations in this isoform were shown to correlate with inherited cardiac arrhythmias [18]. The dominant-negative effect of the inactive K_vLQT_1 isoform is abolished in the presence of the β-subunit IsK [18]. By analogy, similar roles could be assumed for the inactive *h*SK3 isoforms, *h*SK3-1B and *h*SK3_ex1c. In addition the existence of an as yet unknown β-subunit could also be assumed, which influences the dominant-negative effect of *h*SK3-1B and *h*SK3_ex1c.

In principle, the current reduction in the experiments with *h*SK3 channels co-expressed with *h*SK3_ex1c could be due to the fact that *h*SK3_ex1c subunits, although non-functional, could still bind calmodulin. SK channel activation has been shown to be mediated by calmodulin, which constitutively binds to the C-terminus of SK channel subunits [2-4]. This binding of calmodulin to *h*SK3-ex1c subunits would compete with calmodulin-*h*SK3 channel interaction resulting in less functional *h*SK3 channels that could be activated by Ca^{2+} binding to calmodulin. However, in the experiments with the *h*SK3-eGFP, we observed an approximately 12-fold increase in functional *h*SK3 channels. This suggests that the amount of calmodulin in the cell is sufficient to mediate the activation of such a high number of *h*SK3 channels. The *h*SK3_ex1c subunits would have to bind at least this amount of calmodulin to account for the reduction in functional hSK3 channels via that mechanism. Therefore it seems unlikely that the mechanism of complete current reduction in the co-expression experiments is due to a lack of calmodulin being able to act on *h*SK3 subunits.

An interesting observation is the strongly increased current amplitude in cells expressing *h*SK3-eGFP. We have no explanation for this phenomenon. This effect is due to a higher channel expression level of functional *h*SK3-eGFP channels compared to the wild type channel. One might speculate that the increase in functional channels is due to an increase in protein synthesis or protein stability. Alternatively, the eGFP-tag might stabilize SK3 subunits in the membrane or may increase their transport into the plasma membrane. Contrary to *h*SK3-1B, *h*SK3_ex1c is not expressed in brain tissues, but is expressed in skeletal muscle. Therefore, it could play a role in modulating SK3 whole-cell current amplitude in, for example, skeletal muscle. So far nothing is known about the regulation of the expression of SK3 transcripts. However, the fact that *h*SK3-1B and *h*SK3_ex1c show different tissue distributions implies that their expression might be regulated independently. This could provide a differential modulation of *h*SK3 whole-cell current amplitude. The expression of *h*SK3_ex1c may be the reason why there are no apamin binding sites [19, 20] nor SK3 currents found in adult skeletal muscle [21]. Interestingly, functional SK3 channels are observed after denervation of skeletal muscle and in skeletal muscles of patients with myotonic dystrophy [21-23]. Such an up-regulation of SK3 channel activity might be explained at least in part by an alteration of *h*SK3_ex1c expression and not solely via an up-regulation of *h*SK3 transcripts [22]. The inducible up-regulation of SK3 channels in a transgenic mouse is shown to induce abnormal respiratory response to hypoxic conditions and compromised parturition [24]. A suppression of SK3 channels in the same mouse model leads to an increase of the frequency of phasic urinary bladder smooth muscle contraction [25]. This report is in line with the observation, that the selective blockage of IK1 and SK3 channels suppresses the vasodilation, which is mediated by the endothelium-derived hyperpolarizing factor EDHF [26]. These findings underline the importance of SK3 channel activity as a determinant for smooth muscle contractility. Furthermore, all SK channels are thought to be involved in regulating the glucose-dependent insulin release of pancreatic islet cells [27]. All these findings emphasize the importance of SK3 channel regulation for many physiological events. An additional possibility of SK3 channel regulation beside SK3 channel expression could be important for a more robust fine tuning of cellular function than it is possible solely by an expressional regulation of SK3 channels. Therefore, isoform hSK3_ex1c could play a vital role in many homeostatic processes like smooth muscle contractility and control of blood pressure, in respiratory rhythmogenesis and the control of glucose serum level.

Note added in proof: After acceptance of this manuscript another paper was published describing the identical isoform hSK3_ex1c as hSK3-1C (Kolski-Andreaco AA, Tomita H, Shakkottai VV, Gutman GA, Cahalan MD, Gargus JJ, Chandy KG. *Journal of Biological Chemistry* 2003 Nov24 [Epub ahead of print]) confirming and extending our findings.

References

1 Kohler M, Hirschberg B, Bond CT, Kinzie JM, Marrion NV, Maylie J, Adelman JP: Small-conductance, calcium-activated potassium channels from mammalian brain. Science 1996;273:1709-1714.

2 Fanger CM, Ghanshani S, Logsdon NJ, Rauer H, Kalman K, Zhou J, Beckingham K, Chandy KG, Cahalan MD, Aiyar J: Calmodulin mediates calcium-dependent activation of the intermediate conductance KCa channel, IKCa1. J Biol Chem 1999;274:5746-5754.

3 Keen JE, Khawaled R, Farrens DL, Neelands T, Rivard A, Bond CT, Janowsky A, Fakler B, Adelman JP, Maylie J: Domains responsible for constitutive and Ca^{2+}-dependent interactions between calmodulin and small conductance Ca^{2+}-activated potassium channels. J Neurosci 1999;19:8830-8838.

4 Schumacher MA, Rivard AF, Bachinger HP, Adelman JP: Structure of the gating domain of a Ca^{2+}-activated K+ channel complexed with Ca^{2+}/calmodulin. Nature 2001;410:1120-1124.

5 Xia XM, Fakler B, Rivard A, Wayman G, Johnson-Pais T, Keen JE, Ishii T, Hirschberg B, Bond CT, Lutsenko S, Maylie J, Adelman JP: Mechanism of calcium gating in small-conductance calcium-activated potassium channels. Nature 1998;395:503-507.

6 Sah P: Ca^{2+}-activated K^+ currents in neurones: types, physiological roles and modulation. Trends Neurosci 1996;19:150-154.

7 Sah P, Louise Faber ES: Channels underlying neuronal calcium-activated potassium currents. Prog Neurobiol 2002;66:345-353.

8 Demolombe S, Baro I, Pereon Y, Bliek J, Mohammad-Panah R, Pollard H, Morid S, Mannens M, Wilde A, Barhanin J, Charpentier F, Escande D: A dominant negative isoform of the long QT syndrome 1 gene product. J Biol Chem 1998;20;273:6837-6843.

9 Zhang BM, Kohli V, Adachi R, Lopez JA, Udden MM, Sullivan R: Calmodulin binding to the C-terminus of the small-conductance Ca^{2+}-activated K^+ channel hSK1 is affected by alternative splicing. Biochemistry 2001;40:3189-3195.

10 Shmukler BE, Bond CT, Wilhelm S, Bruening-Wright A, Maylie J, Adelman JP, Alper SL: Structure and complex transcription pattern of the mouse SK1 K(Ca) channel gene, KCNN1. Biochim Biophys Acta 2001;19;1518:36-46.

11 Tomita H, Shakotai VG, Gutman GA, Sun G, Bunney WE, Cahalan MD, Chandy KG, Gargus JJ: Novel truncated isoform of SK3 ptassium channel is a potent dominant-negative regulator of SK currents: implications in schizophrenia. Mol.Psychiatry 2003;8:524-535.

12 Wittekindt OH, Visan VM, Morris-Rosendahl DJ, Grissmer S: A scyllatoxin insensitve isoform of the human hSK3-channel. Biophysical Journal 2003;84:92a.

13 Heinzel SS, Krysan PJ, Calos MP, DuBridge RB: Use of simian virus 40 replication to amplify Epstein-Barr virus shuttle vectors in human cells. J Virol 1988;62:3738-3746.

14 DuBridge RB, Tang P, Hsia HC, Leong PM, Miller JH, Calos MP: Analysis of mutation in human cells by using an Epstein-Barr virus shuttle system. Mol Cell Biol 1987;7:379-387.

15 Hamill OP, Marty A, Neher E, Sakmann B, Sigworth FJ: Improved patch-clamp techniques for high-resolution current recording from cells and cell-free membrane patches. Pflugers Arch 1981;391:85-100.

16 Grunnet M, Jespersen T, Angelo K, Frokjaer-Jensen C, Klaerke DA, Olesen SP, Jensen BS: Pharmacological modulation of SK3 channels. Neuropharmacology 2001;40:879-887.

17 Pereon Y, Demolombe S, Baro I, Drouin E, Charpentier F, Escande D: Differential expression of KvLQT1 isoforms across the human ventricular wall. Am J Physiol Heart Circ Physiol 2000;278:H1908-H1915.

18 Mohammad-Panah R, Demolombe S, Neyroud N, Guicheney P, Kyndt F, van den Hoff M, Baro I, Escande D: Mutations in a dominant-negative isoform correlate with phenotype in inherited cardiac arrhythmias. Am J Hum Genet 1999;64:1015-1023.

19 Behrens MI, Jalil P, Serani A, Vergara F, Alvarez O: Possible role of apamin-sensitive K^+ channels in myotonic dystrophy. Muscle Nerve 1994;17:1264-1270.

20 Renaud JF, Desnuelle C, Schmid-Antomarchi H, Hugues M, Serratrice G, Lazdunski M: Expression of apamin receptor in muscles of patients with myotonic muscular dystrophy. Nature 1986;319:678-680.

21 Pribnow D, Johnson-Pais T, Bond CT, Keen J, Johnson RA, Janowsky A, Silvia C, Thayer M, Maylie J, Adelman JP: Skeletal muscle and small-conductance calcium-activated potassium channels. Muscle Nerve 1999;22:742-750.

22 Kimura T, Takahashi MP, Okuda Y, Kaido M, Fujimura H, Yanagihara T, Sakoda S: The expression of ion channel mRNAs in skeletal muscles from patients with myotonic muscular dystrophy. Neurosci Lett 2000;295:93-96.

23 Ramirez BU, Behrens MI, Vergara C: Neural control of the expression of a Ca^{2+}-activated K^+ channel involved in the induction of myotonic-like characteristics. Cell Mol Neurobiol 1996;16:39-49.

24 Bond CT, Sprengel R, Bissonnette JM, Kaufmann WA, Pribnow D, Neelands T, Storck T, Baetscher M, Jerecic J, Maylie J, Knaus HG, Seeburg PH, Adelman JP: Respiration and parturition affected by conditional overexpression of the Ca^{2+}-activated K^+ channel subunit, SK3. Science 2000;289:1942-1946.

25 Herrera GM, Pozo MJ, Zvara P, Petkov GV, Bond CT, Adelman JP, Nelson MT: Urinary bladder instability induced by selective suppression of the murine small conductance calcium-activated potassium (SK3) channel. J Physiol 2003;551:893-903.

26 Eichler I, Wibawa J, Grgic I, Knorr A, Brakemeier S, Pries AR, Hoyer J, Kohler R: Selective blockade of endothelial Ca^{2+}-activated small- and intermediate-conductance K^+-channels suppresses EDHF-mediated vasodilation. Br J Pharmacol 2003;138:594-601.

27 Tamarina NA, Wang Y, Mariotto L, Kuznetsov A, Bond C, Adelman J, Philipson LH: Small-conductance calcium-activated K^+ channels are expressed in pancreatic islets and regulate glucose responses. Diabetes 2003;52:2000-2006.